GSA Data Repository 2016029

Data repository for: Surface roughness dating of long-runout landslides near Oso, WA reveals persistent postglacial hillslope instability

Sean R. LaHusen[1], Alison R. Duvall[1], Adam M. Booth[2], and David R. Montgomery[1]

[1]Department of Earth and Space Sciences, University of Washington, Box 351310, Seattle, Washington 98195, USA

[2]Department of Geology, Portland State University, 1721 SW Broadway, Portland, Oregon, 97201 USA

This study applies a new regional approach to dating landslide deposits that combines large-scale geomorphic analysis of LiDAR imagery with absolute age dating of selected landslides in order to predict ages of all landslides across the study area.

Landslide Mapping and Characterization

We mapped all landslides within a ~6km long section of the North Fork Stillaguamish River valley, directly surrounding the catastrophic 2014 Oso Landslide (Fig. DR1). Landslides were mapped from 0.9m resolution LiDAR bare-earth imagery acquired by the Washington State Department of Transportation (2014).

The criteria we used to map landslide units were the presence of an arcuate headscarp overlying a hummocky portion of terrain with evidence of displacement in a down-gradient direction. This LiDAR data was also used for additional geomorphometric analyses of each landslide deposit, including standard deviation of slope (a measure of surface roughness), total

height, and total length (Table DR1). We then verified digitally mapped landslides in the field by examining exposed deposit stratigraphy and surface morphology.

Delineating landslide units proved challenging when considering remobilization of landslide deposits. The criteria we used to separate a landslide into 2 events (an initial failure and a secondary remobilization of the original landslide material) was the presence of a large (tens of meters) secondary scarp that extended continuously across the entire width of the landslide deposit. Moreover, this scarp must appear sharper, steeper, and overall morphologically distinct from other extensionally faulted blocks within the landslide deposit and from the main upper headscarp formed by the initial landslide. If these criteria are met, we feel more confident that the material below this secondary scarp is a younger failure whose timing is substantially different from the timing of the first failure. Using these criteria, for example, the 2014 Oso Landslide would not be considered two events because the upper block is not separated from the lower portion of the landslide mass by a continuous, sharp scarp, but rather a series of laterally discontinuous extensional faults, while the Headache Creek landslide would.

To characterize landslide morphology, we used ESRI ArcMap 10 software to measure individual landslide headscarp dimensions, deposit area, and H:L, where H is defined as the elevation difference between the top of the headscarp and the base of the landslide deposit at the toe and L as the length from the headscarp to the distal edge of the landslide toe (Supplementary Table DR 1).

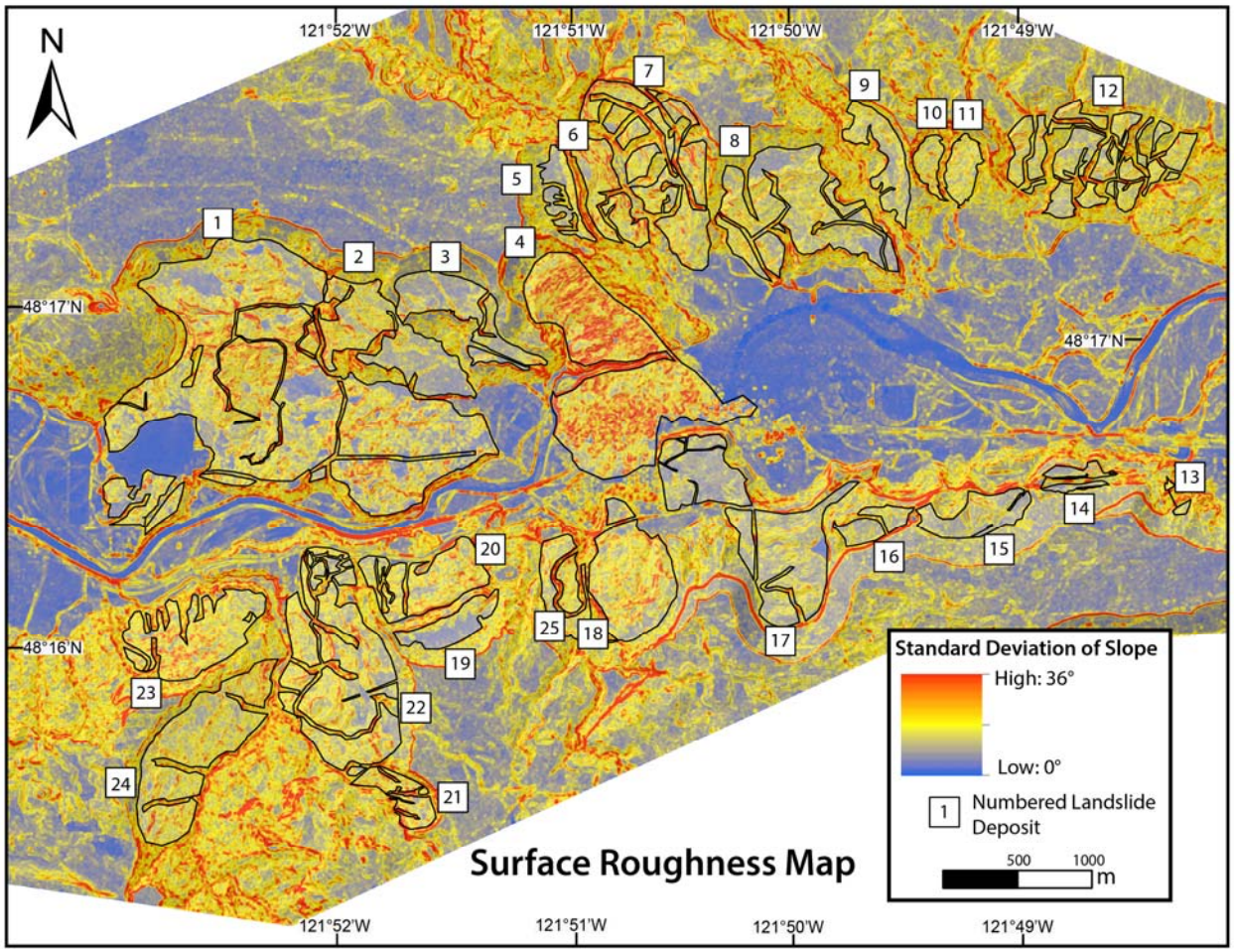

Figure DR1. Map showing surface roughness of mapped landslide polygons across the study area. Land surface is colored by standard deviation of slope (SDS), ranging from low SDS shown in blue (0°) to high SDS shown in red (up to 36°). Opaque landslide polygons used in roughness analysis are numbered, and correspond with numbers in Table DR1. These polygons reflect the removal of roads, gullies, and fluvial erosive contacts from the landslide polygons displayed in Figure 3.

Table DR1: Morphological attributes and estimated age for each landslide.

ID #	Name	Area (km^2)	Headscarp height (m)	Height (m)	Length (m)	H:L Ratio	SDS (°)	Estimated age (YBP) from roughness-age function
1	Rowan Landslide	1.99	90	200	1980	0.10	5.72	1200
2		0.33	100	180	910	0.20	5.11	2800
3		0.28	90	190	790	0.24	4.40	7500
4	2014 Oso Landslide	0.94	110	190	2000	0.10	8.02	50
5	Headache Creek Landslide	0.27	70	140	580	0.24	4.57	5900
6		0.13	20	60	220	0.27	7.16	160
7		0.42	20	130	410	0.32	6.30	530
8		0.57	50	160	910	0.18	5.13	2700
9		0.14	30	90	300	0.30	5.09	2800
10		0.04	10	70	200	0.35	6.10	700
11		0.07	30	90	340	0.26	5.81	1000
12		0.47	20	160	620	0.26	5.53	1600
13		0.06	90	150	440	0.34	5.55	1500
14		0.15	110	160	460	0.35	4.38	7700
15		0.26	100	160	580	0.28	4.46	7000
16		0.14	110	150	460	0.33	4.60	5700
17		0.56	80	180	1400	0.13	4.19	10000
18		0.47	90	130	1010	0.13	6.13	670
19		0.12	60	160	730	0.22	4.04	12000
20		0.21	30	100	460	0.22	6.26	560
21		0.07	30	70	240	0.29	6.96	210
22		0.58	50	150	790	0.19	5.72	1200
23		0.32	40	160	550	0.29	6.57	360
24		0.31	40	120	490	0.24	6.08	710
25		0.03	15	40	160	0.25	6.47	420

Surface Roughness Analysis

To measure surface roughness for each mapped landslide unit, we calculated average standard deviation of slope (SDS) from the LiDAR data using a 15m x 15m roving window in ArcMap 10. To remove the effect of increased roughness from gullying, all gullies incised more than 2m into landslide deposits were removed manually from the digitally mapped landslide polygons so they would not affect the roughness analysis (Fig. DR1). Other roughness biases, such as headscarps, roads, and modern NFS River erosional contacts, were also removed prior to the

analysis so that only the natural landslide deposit surfaces were measured. SDS was calculated for each cell in the study area, then, an average value of SDS was determined for each of the 25 mapped landslide polygons (Fig. DR1). This average SDS value is used to estimate landslide age using our calibrated roughness-age curve.

Radiocarbon Dating

Radiocarbon ages of woody debris provided absolute ages for the Rowan and Headache Creek landslides (Table DR2). Wood samples are interpreted to be from trees killed during the landslide event, and therefore represent maximum landslide age. The age of the Rowan Landslide was determined using new carbon dates from six samples of woody debris entrained at different sites within the landslide deposit; four from the toe (Samples 1-4 in Fig. 1; Table DR2) and two from the main body of the slide (Samples 4,5 in Fig. 1; Table DR2). These ages place bounds on the timing of failure of this landslide between 300-694 yr cal BP (from lower end 1σ error range of youngest sample age to upper 1σ error range of oldest sample age). The age span in this dataset reflects the sampling of old growth trees in the slide deposit. Samples were not all intact trunks, so that we were not always sure where within the tree trunk the sample originated. When sampling woody debris from an old growth forest that was disrupted and entrained in the land slide mass, a span of a few hundred years is not surprising. Samples from the toe were excavated from exposed landslide deposit within cutbanks along the NFS River, whereas samples from the main body were found protruding from the wall of a 5m deep stream gully incised into the landslide deposit. Three radiocarbon dates from bark collected off of buried logs exposed in the eastern margin of the 2014 Oso Landslide (Keaton, et al., 2014) constrain the timing of the Headache Creek Landslide to 5757-6278 yr cal BP (Samples 8-10 in Fig. 1; Table

DR2). All wood samples were analyzed at AMS Direct in Bothell, WA, and then calibrated using OxCal 4.2 software (Ramsey, 2009).

Table DR2: Radiocarbon dating results

Sample #	Sample Material	Deposit Type	Radiocarbon Age (1σ error)	Yr cal BP (1σ error)	Location (Long;Lat)
1	Wood (broken branch)	Rowan landslide	572±37	524-651	-121.879; 48.272
2	Wood (trunk fragment)	Rowan landslide	307±30	300-464	-121.877; 48.272
3	Wood (trunk fragment)	Rowan landslide	722±24	653-694	-121.869; 48.274
4	Wood (trunk fragment)	Rowan landslide	693±24	565-683	-121.869; 48.274
5	Bark (intact trunk)	Rowan landslide	368±23	319-500	-121.876; 48.283
6	Wood (outer trunk)	Rowan landslide	426±29	334-526	-121.876; 48.283
7	Wood (outer trunk)	Fluvial terrace buried by Rowan landslide	10,103±37	11,406-11,978	-121.858; 48.274
8	Bark (intact tree trunk)	Headache Creek landslide	5304 ±28	5995-6182	-121.850; 48.287
9	Bark (intact tree trunk)	Headache Creek landslide	5371 ±28	6019-6278	-121.849; 48.286
10	Bark (intact tree trunk)	Headache Creek landslide	5138 ±27	5757-5983	-121.848; 48.286

Calibrated Ages from Surface Roughness Curve

We plot radiometric carbon dates of landslide deposits against a quantitative analysis of surface roughness (Fig. 2). To determine what type of regression to use to calibrate the age-roughness curve, we applied a linear diffusive landscape evolution model to the Oso landslide deposit which has an initial age of zero. The numerical model simulated the change in the land surface elevation, z, with time, t, as $\partial z/\partial t = D\nabla^2 z$, where D is a constant. Using a LiDAR digital elevation model of the 2014 Oso landslide deposit as the initial condition, we integrated

this equation forward in time using an alternating-direction implicit method (Press, 2007), and measured SDS of the landslide deposit at each time step. A value of $D = 0.001$ m^2/yr resulted in the minimum root mean square misfit between the modeled surface roughness and observed surface roughness for the four data points in the age-roughness calibration curve (Fig. 2), and both the observed and modeled age vs. roughness curves are well-fit by exponential functions.

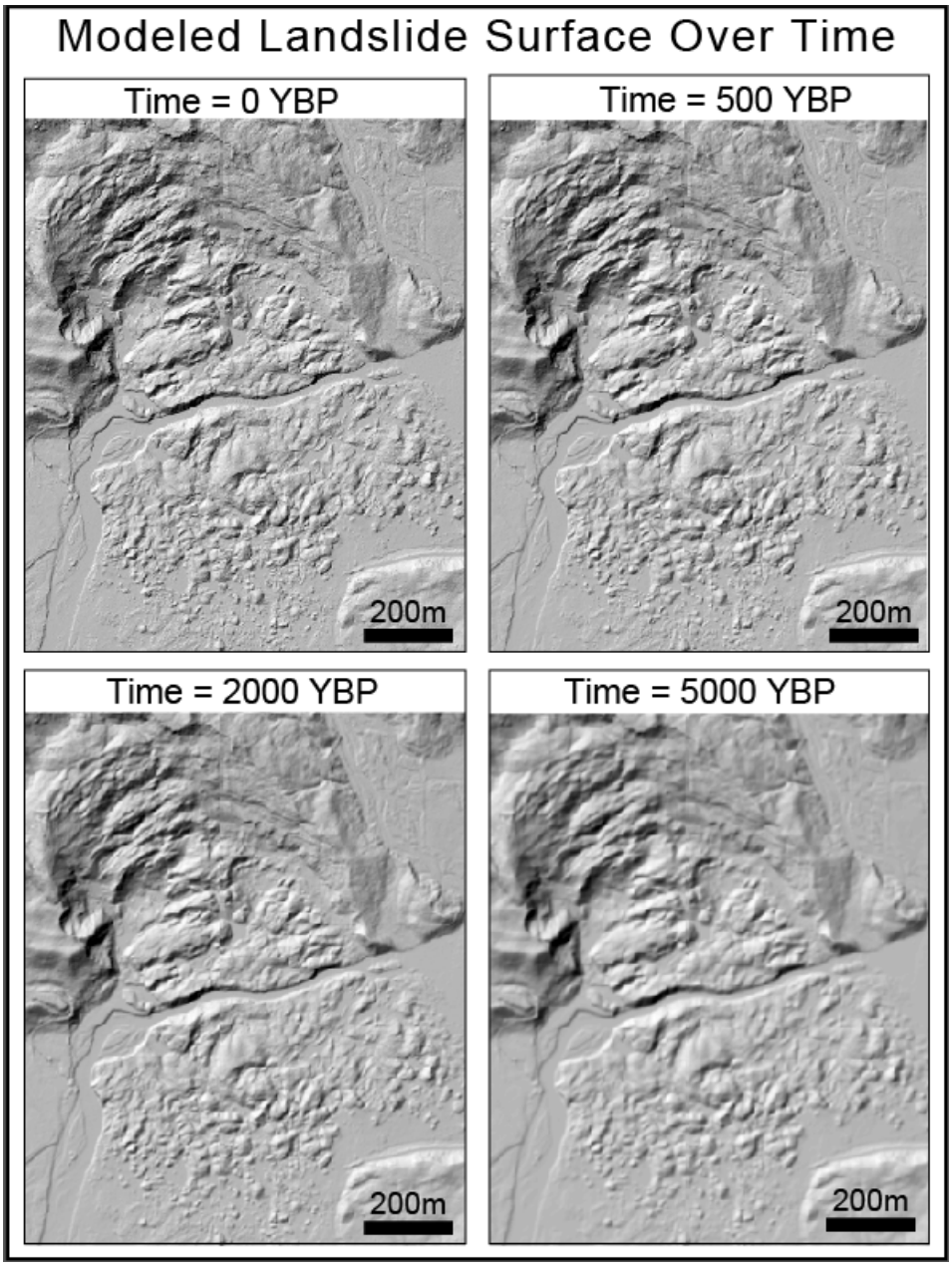

Figure DR2. Hillshade images showing the modeled evolution of the Oso Landslide surface topography at time 0 years, 500 years, 2000 years, and 5000 years.

We then fit a single exponential regression to the observed age-roughness plot (Fig. 2b) using Sigma Plot software, and use this function to estimate the age of the other mapped landslides across the study area for which absolute age information does not exist. Observed SDS ranges from 4.04 to 8.02 degrees within the study area, which corresponds to estimated ages from 50 to 12,000 ybp using the best-fit function (Table DR1).

Potential Sources of Error

Perhaps the most significant potential for error stems from the challenge of using morphology to date landslide complexes that may have mobilized multiple times. It is important to note that even if our landslide delineation of younger and older events within a complex is 100% accurate, the earliest landslide could appear to be older than it may actually be. This could occur if the lower portion of the earlier landslide was rougher, but because it has remobilized it is considered a separate event, and is excluded from the roughness analysis of the earlier landslide. While this may be a potential source of error, it is only likely to make a landslide appear older, not younger, making any error in age estimation likely to fall on the conservative side.

While many of the landslides in the study area share similar morphology, there is some variability in H:L and deposit area. To explore whether failure mechanics could add some complexity to our method, we measured the standard deviation of slope of the pre-Oso landslide (known as the Hazel Landslide, which has a protracted and complex history of activity) Standard deviation of slope (SDS) values from the 2006 Hazel slide are less than that of the longer runout 2014 Oso Landslide (6.4 degrees compared to 8.0 degrees), however, this difference is not sufficient to place it in a different age class. As the Hazel landslide is the only example of a slope failure with LiDAR data that we can compare against the 2014 Oso Landslide, we hesitate to

recognize this as a landscape-wide bias. To consider this potential issue over the entire dataset, we plot landslide area and H:L ratio against calculated standard deviation of slope (Fig. DR3). These plots show no correlation between area or H:L and SDS for the landslides this study concerns (R^2 values of 0.02 for both plots).

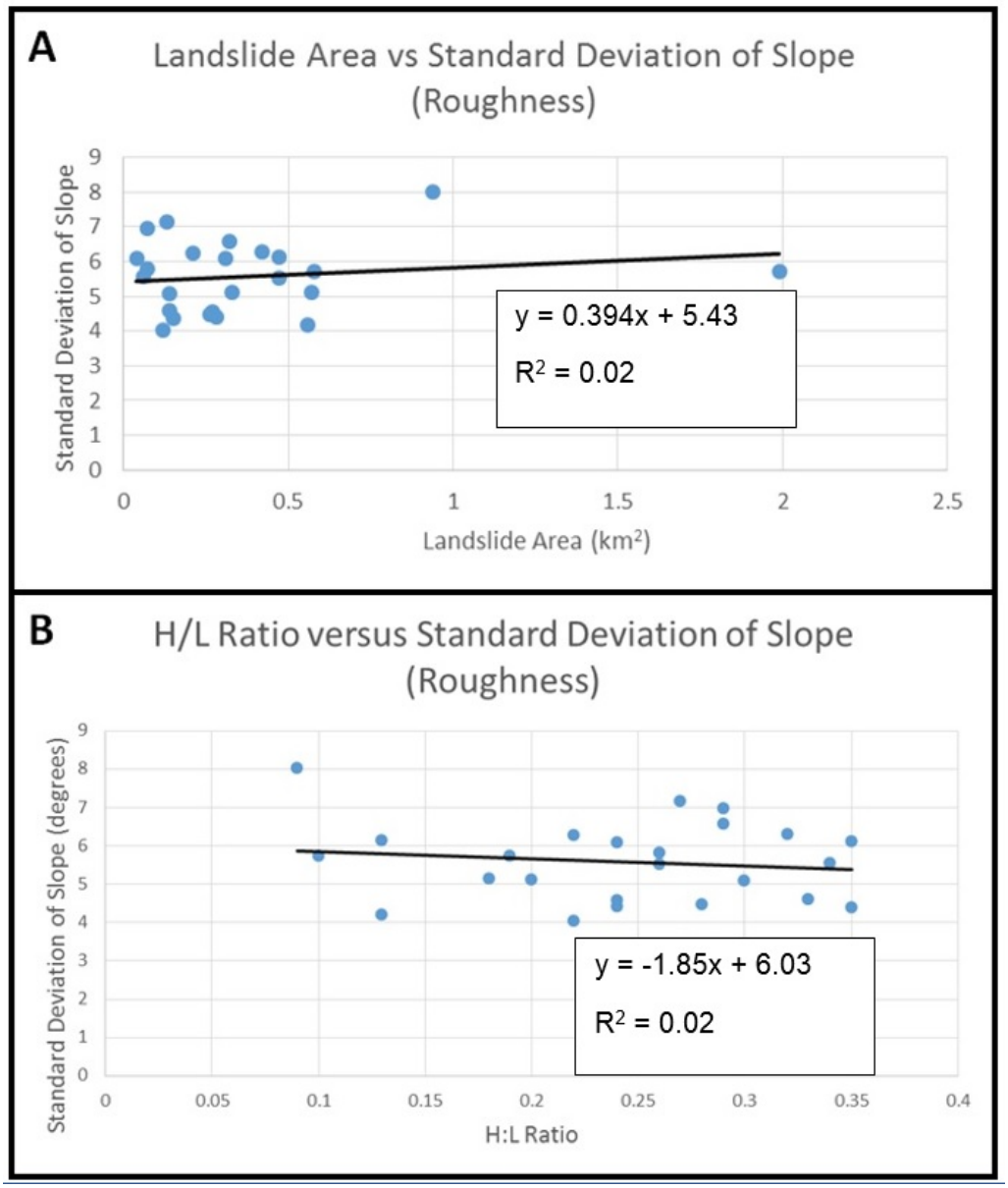

Figure DR3. Graph of landslide area versus standard deviation of slope (A) and landslide H:L ratio versus standard deviation of slope (B) for all landslides in the study area, with linear trendlines fit to both. Neither graph shows a correlation (R^2 values of 0.02).

References

Keaton, J. R., et al., 2014, The 22 March 2014 Oso Landslide, Snohomish County, Washington. Geotechnical Extreme Events Reconnaissance Association Report **GEER-036**.

Press, W.H., Teukolsky, S.A., Vetterling, W.T., and Flannery, B.P., 2007, Numerical Recipes, 3rd Edition: The Art of Scientific Computing: Cambridge, NY, Cambridge University Press.

Ramsey, C. B., 2009, Bayesian analysis of radiocarbon dates. *Radiocarbon* **51,** 337-360.

Washington State Department of Transportation, 2014, Oso Landslide/Stillaguamish River LiDAR. Puget Sound LiDAR Consortium.